

MODELLING OF CONCRETE CRACKING FOR THE DESIGN OF SHM SYSTEMS: COMPARISON OF IMPLICIT GRADIENT DAMAGE MODELS AND SIMPLIFIED LINEAR REPRESENTATIONS

Maik Brehm*, Thierry J. Massart* AND Arnaud Deraemaeker*

*Université Libre de Bruxelles, BATir - Structural and Material Computational Mechanics
50 av F.D. Roosevelt, CP 194/2, 1050 Bruxelles, Belgium
e-mail: maik.brehm@ulb.ac.be, <http://batir.ulb.ac.be>

Key words: concrete cracking, simplified damage modelling, structural health monitoring

Abstract. It has been commonly agreed that the crack propagation within concrete structures can be realistically simulated by non-local damage models. Due to their low complexity and computational cost, simplified damage models are frequently used in virtual testing calculations of structural health monitoring applications. This contribution aims at justifying the application of such simplified damage models for early damage states.

1 INTRODUCTION

In the last three decades, the interest in modelling local damage phenomena increased continuously, which triggered the development of several damage models for various materials. Available methods for concrete structures are reviewed in [1] and [2]. For concrete structures, continuum damage models are often used compared to discrete crack models, as during the initiation phase of concrete cracks the damage zone is larger than the discrete fully established crack. The non-local damage model developed in [3] and the equivalent implicit gradient damage model (e.g., [4]) are both appropriate for a realistic modelling of crack propagation in concrete together with the accompanying crack process zone. A typical problem of complex damage models is the appropriate definition or identification of several model parameters. Some parameters are related to physical phenomena, other parameters are necessary to stabilise numerically the problem. In addition, such damage propagation calculations remain computationally very expensive.

In the structural health monitoring commu-

nity, virtual tests are frequently performed to design and optimise damage sensitive features to monitor continuously the health of the structure. However, advanced fracture mechanics models are rarely applied. Usually, simplifications based on linear material models with reduced Young's modulus of the whole cross section are used to simulate a certain damage. Examples can be found in [5], [6], and [7]. Deraemaeker [8] first applied an advanced fracture mechanical damage model to investigate the performance of a damage indicator based on dynamic strains. Following this idea, other investigations were performed using an implicit gradient damage law to obtain realistic damage patterns for a notched [9] and a simply supported plain concrete beam [10].

In this paper, a comparison between simplified methods based on partial stiffness reductions of a linear model and the more advanced nonlinear damage propagation calculation based on the implicit gradient damage law is conducted. The results show that under certain conditions very simple damage pattern descriptions can be applied without significant

loss of accuracy in global, as well as, in the local behaviour of the structure under static loading conditions.

2 IMPLICIT GRADIENT DAMAGE LAW

The classical stress-strain relation of elasticity based damage mechanics at a certain point in the structure reads

$$\boldsymbol{\sigma} = (1 - D(\kappa))\mathbf{C}\boldsymbol{\varepsilon}, \quad (1)$$

where $\boldsymbol{\sigma}$ and $\boldsymbol{\varepsilon}$ are the stress and strain tensor and \mathbf{C} the linear elastic material tensor, which is defined in matrix format for a plane-stress state as

$$\mathbf{C} = \frac{E}{1 - \nu^2} \begin{bmatrix} 1 & \nu & 0 \\ \nu & 1 & 0 \\ 0 & 0 & \frac{1-\nu}{2} \end{bmatrix} \quad (2)$$

with the Young's modulus E and the Poisson ratio ν . The damage function value $D(\kappa)$ is set to zero, for undamaged materials. By increasing $D(\kappa)$, a damage growth is in general possible, depending on the previous stress-strain-history. Whether a damage growth is possible or not is defined by the damage loading function

$$f(\bar{\varepsilon}, \kappa) = \bar{\varepsilon} - \kappa, \quad (3)$$

with a positive nonlocal equivalent strain measure $\bar{\varepsilon}$ and a strain related threshold variable κ . For quasi-brittle damage, the Kuhn-Tucker relation needs to be fulfilled in addition

$$f \leq 0, \quad \dot{\kappa} \geq 0, \quad \text{and} \quad \dot{\kappa}f = 0. \quad (4)$$

Therefore, κ needs to be adjusted to guarantee that the equivalent strain measure $\bar{\varepsilon}$ is never larger than than κ , that the value of κ can never decrease, and that an increase of the threshold value κ is only possible with $\kappa = \bar{\varepsilon}$.

Assuming an exponential softening law, the damage function is defined as follows

$$D(\kappa) = \begin{cases} 1 - \frac{\kappa_0}{\kappa} (1 - \alpha + \alpha e^{-\beta(\kappa - \kappa_0)}) & : \kappa > \kappa_0 \\ 0 & : \kappa \leq \kappa_0 \end{cases}, \quad (5)$$

in which κ_0 defines the initial linear elastic domain in terms of equivalent strains.

One possible local equivalent strain definition is the modified von-Mises definition

$$\tilde{\varepsilon} = \frac{k-1}{2k(1-2\nu)} I_1 + \frac{1}{2k} \sqrt{\frac{(k-1)^2}{(1-2\nu)^2} I_1^2 + \frac{2k}{(1+\nu)^2} J_2} \quad (6)$$

according to [11]. Assuming a 2D plane stress formulation, the first invariant of the strain tensor and the second invariant of the deviatoric strain tensor are

$$\begin{aligned} I_1 &= \frac{1-2\nu}{1-\nu} (\varepsilon_{xx} + \varepsilon_{yy}) \quad \text{and} \\ J_2 &= 2(\varepsilon_{xx}^2 + \varepsilon_{yy}^2 - \varepsilon_{xx}\varepsilon_{yy}) + 1.5\varepsilon_{xy}^2 + \\ &\quad + \frac{2\nu}{(1-\nu)^2} (\varepsilon_{xx} + \varepsilon_{yy})^2, \end{aligned} \quad (7)$$

respectively. The parameter $k = \frac{f_c}{f_t}$ allows accommodating different values for tensile strength f_t and compression strength f_c , which makes this local equivalent strain formulation suitable for concrete.

Based on local equivalent strains $\tilde{\varepsilon}(\mathbf{y})$ at certain positions \mathbf{y} of the structure, a nonlocal equivalent strain

$$\bar{\varepsilon}(\mathbf{x}) = \frac{1}{\Psi(\mathbf{x})} \int_{\tilde{\Omega}} \psi(\mathbf{y}; \mathbf{x}) \tilde{\varepsilon}(\mathbf{y}) d\Omega \quad (8)$$

with

$$\Psi(\mathbf{x}) = \int_{\tilde{\Omega}} \psi(\mathbf{y}; \mathbf{x}) d\Omega \quad (9)$$

can be defined, thanks to which the local equivalent strains $\tilde{\varepsilon}(\mathbf{y})$ are averaged over a certain volume $\tilde{\Omega}$. The weighting function $\psi(\mathbf{y}; \mathbf{x})$ guarantees that local equivalent strains $\tilde{\varepsilon}(\mathbf{y})$ close to the position \mathbf{x} have a higher weight to the nonlocal equivalent strain $\bar{\varepsilon}(\mathbf{x})$ than local equivalent strains related to the boundary of the volume $\tilde{\Omega}$.

After substitution of the Taylor expansion of $\tilde{\varepsilon}(\mathbf{y})$ into the Equation (8), a differential equation

$$\bar{\varepsilon}(\mathbf{x}) = \tilde{\varepsilon}(\mathbf{x}) + c_i \frac{\delta^2 \tilde{\varepsilon}}{\delta x_i^2} + c_{ij} \frac{\delta^4 \tilde{\varepsilon}}{\delta x_i^2 \delta x_j^2} + \dots \quad (10)$$

can be obtained, which reduces to

$$\bar{\varepsilon}(\mathbf{x}) = \tilde{\varepsilon}(\mathbf{x}) + c\nabla^2\tilde{\varepsilon}(\mathbf{x}) \quad (11)$$

by neglecting higher order terms. Applying the Laplacian operator to Equation (11) and neglecting again higher order terms, it yields

$$c\nabla^2\bar{\varepsilon}(\mathbf{x}) = c\nabla^2\tilde{\varepsilon}(\mathbf{x}). \quad (12)$$

Finally, the Equation

$$\bar{\varepsilon}(\mathbf{x}) - c\nabla^2\bar{\varepsilon}(\mathbf{x}) = \tilde{\varepsilon}(\mathbf{x}) \quad (13)$$

can be derived, by subtracting Equation (12) from (11). Hence, the nonlocal strain is given as the solution of the boundary value problem consisting of the Helmholtz equation (13) and appropriate boundary conditions. Further explanations can be found in [4].

3 SIMPLIFIED LINEAR REPRESENTATION

3.1 General idea

The previously described damage law is suitable for the calculation of damage propagation in plain concrete. For each stress-strain-state, the damage function values $D(\kappa)$ defined for each integration point of all elements are calculated. If someone is only interested in one single specific stress-strain-state, the complex nonlinear finite element model can be replaced by an ordinary linear finite element model, if the damage function values $D(\kappa)$ are known for every integration point i of all elements.

Without loss of generality of the proposed approach, it is assumed that the finite element model consists of 9-node quadrilateral plane finite elements using a 3 by 3 Gauss point integration scheme. For each integration point, a different damage function value $D_{(i)} = D_{(i)}(\kappa)$ can be obtained. All other constitutive law parameters are defined to be constant for all 9 integration points i . Therefore, the secant element stiffness matrix can be derived by Gauss point integration

$$\mathbf{K}_s = \sum_{i=1}^9 (1 - D_{(i)}) \mathbf{B}_{(i)}^T \mathbf{C} \mathbf{B}_{(i)} \det \mathbf{J}_{(i)} w_{(i)} t_{(i)} \quad (14)$$

in which $w_{(i)}$, $\mathbf{J}_{(i)}$, $t_{(i)}$, $\mathbf{B}_{(i)}$ are the weighting coefficients of the Gaussian points, the Jacobian matrix, the thickness of the element, and the strain-displacement-matrix, respectively.

Using this secant element stiffness matrix \mathbf{K}_s for each element, the linear unloading and reloading path of the nonlinear finite element model can be exactly represented with the ordinary linear finite element model. This can be realised by defining the Young's modulus of each integration point and element by $E_{dam(i)} = (1 - D_{(i)})E$. Of course, most standard finite element codes do not support the option to define the Young's modulus individually for each integration point of an element. Hence, a possibility is needed to assign a suitable constant damage function value $D_{(i)} = \tilde{D} \forall i$ for all integration points within each element to obtain the Young's modulus

$$E_{dam} = (1 - \tilde{D})E \quad (15)$$

related to damaged elements. In the following subsections, several methods are discussed.

3.2 Averaging of damage function values

Assuming the 9 damage function values $D_{(i)}$ per element serve as support points for a regression model, several pairs of polynomials can be used to find a regression surface. One possibility is to use interpolation functions $\mathbf{h}(\xi, \eta) = [h_1(\xi, \eta) \ h_2(\xi, \eta) \ \dots]^T$ defined in the natural coordinates (ξ, η) as typically applied for displacement interpolation in finite element formulations. With the matrices

$$\mathbf{A} = \sum_i \det \mathbf{J}_{(i)} w_{(i)} t_{(i)} \mathbf{h}(\xi_{(i)}, \eta_{(i)})^T \mathbf{h}(\xi_{(i)}, \eta_{(i)}) \quad (16)$$

and

$$\mathbf{y} = \sum_i \det \mathbf{J}_{(i)} w_{(i)} t_{(i)} \mathbf{h}(\xi_{(i)}, \eta_{(i)})^T D_{(i)} \quad (17)$$

equation

$$\mathbf{A}\mathbf{x} = \mathbf{y} \quad (18)$$

can be solved in a least squares sense with respect to the regression coefficients \mathbf{x} . The new regression surface is then defined by

$$f(\xi, \eta) = \mathbf{h}(\xi, \eta)^T \mathbf{x} \quad (19)$$

at every point (ξ, η) in the natural coordinate system.

As a constant approximation of the damage function value is of interest, an interpolation function $\mathbf{h} = h_1 = 1 \forall (\xi, \eta)$ is chosen. The scalar value $\mathbf{x} = \tilde{D}_a$ is a constant average of the damage function value distribution within one element, which can be applied in Equation (15). In contrast to the subsequent methods, no iteration is needed, which makes this approach computationally very efficient and robust.

3.3 Optimised damage function value

To obtain an optimal damage function value constant for all integration points of the element, three different objective functions are proposed. The first objective function is related to the Frobenius norm of the differences of stiffness matrices related to the secant stiffness \mathbf{K}_s according to Equation (14) and the stiffness matrix

$$\mathbf{K}_c(\tilde{D}) = \sum_{i=1}^9 (1-\tilde{D}) \mathbf{B}_{(i)}^T \mathbf{C} \mathbf{B}_{(i)} \det \mathbf{J}_{(i)} w_{(i)} t_{(i)} \quad (20)$$

obtained by a constant damage function value \tilde{D} . Hence, the optimal value is given by

$$\tilde{D}_k = \operatorname{argmin}_{\tilde{D}} \|\mathbf{K}_s - \mathbf{K}_c(\tilde{D})\|_F. \quad (21)$$

A criterion, which considers the strain distribution, can be defined based on the Euclidean norm of the differences between the internal forces

$$\mathbf{r}_s = \mathbf{K}_s \mathbf{d}_s \quad (22)$$

related to the secant stiffness and

$$\mathbf{r}_c(\tilde{D}) = \mathbf{K}_c(\tilde{D}) \mathbf{d}_s \quad (23)$$

using the displacements of each element node assembled in the vector \mathbf{d}_s , which are obtained from the finite element model applying the secant element matrices \mathbf{K}_s . The optimality criterion is then defined by

$$\tilde{D}_r = \operatorname{argmin}_{\tilde{D}} \|\mathbf{r}_s - \mathbf{r}_c(\tilde{D})\|_2. \quad (24)$$

Another criterion is the potential energy of the element under deformation. Based on the differences of the elastic potential energy related to the secant stiffness

$$\Pi_s = \frac{1}{2} \mathbf{d}_s^T \mathbf{K}_s \mathbf{d}_s \quad (25)$$

and the elastic potential energy assuming a constant damage function value within the element

$$\Pi_c(\tilde{D}) = \frac{1}{2} \mathbf{d}_s^T \mathbf{K}_c(\tilde{D}) \mathbf{d}_s, \quad (26)$$

the optimal constant damage function value can be obtained by

$$\tilde{D}_\pi = \operatorname{argmin}_{\tilde{D}} \|\Pi_s - \Pi_c(\tilde{D})\|_2. \quad (27)$$

The optimal damage function values are assembled in Equation (15) to defined the reduced Young's modulus of each element.

3.4 Artificial damage pattern

The previously described approaches assume that size and area of the damage pattern are known for each element. If no detailed information about the geometry of the damage pattern is available, a global damage pattern needs to be defined artificially as realistic as possible. The parameters, which describe this damage pattern can be, for example, calibrated by means of a global load-deflection-curve, as done in this study.

A common approach for an artificial damage pattern is to distribute the damage equally across the whole cross-section within a certain width. In this case, the expansion of the damage is predefined and the normalised value of damage $\tilde{D}_v \in [0, 1]$ can be adjusted. The value \tilde{D}_v can be directly applied in Equation (15) to calculate the reduced Young's modulus of the elements within the predefined damaged area.

If the damage path is approximately known, the damage propagation can be described by few variables. In this study, only one variable $\lambda \in [0, 1]$ is applied to define the damage propagation. The variable λ indicates the crack length within the normalised section height. All elements within the described damaged area are assumed to be completely damaged. Hence,

$\tilde{D}_\lambda = 1$ is assembled in Equation (15) for those elements.

Figures 1 and 2 depict the approach in case of a single crack and Figures 3 and 4 show an example in case of multiple cracks within a beam structure. For multiple cracks a predefined function $f(x)$ is introduced to define the damage distribution for each crack depending on its position x within the structure.

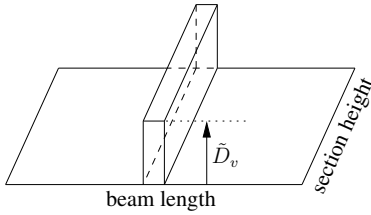


Figure 1: Definition of damage pattern with variable damage value \tilde{D}_v and predefined constant damaged area in case of one crack.

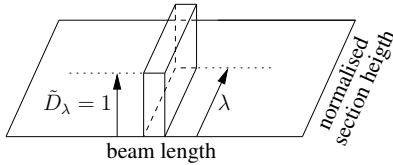


Figure 2: Definition of damage pattern with variable damage length λ and a predefined constant damage width and damage severity $\tilde{D}_\lambda = 1$ in case of one crack.

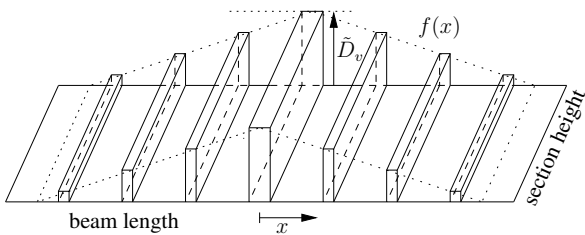


Figure 3: Example of damage pattern definition with variable damage value \tilde{D}_v and predefined constant damaged areas in case of multiple cracks.

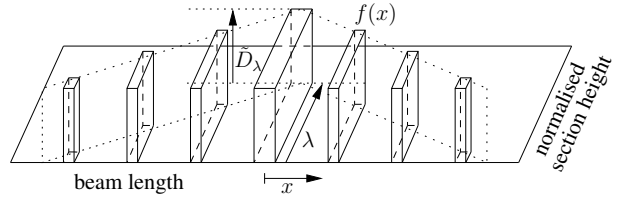


Figure 4: Example of damage pattern definition with variable damage length λ and predefined constant damage widths and damage severity $\tilde{D}_\lambda = 1$ in case of multiple cracks.

4 BENCHMARK: NOTCHED BEAM

4.1 System description

The study is related to a notched beam under three point loading as described in Figure 5. The experimental results are presented in [12], whereas the procedure to identify the uncertain damage and constitutive law parameters was conducted in [9], where the difference between the experimentally obtained and numerically derived global load-deflection-curve has been minimised. The deflections are related to the vertical displacements in the centre of the beam. In the present study, only one possible parameter set is chosen, which is related to the second run using the objective function W_1 based on the Euclidean norm with a constant variable $l_c = 1\text{mm}$ related to the descriptions in [9]. The material and damage law parameters are given in Table 1. The finite element model, applied in this study, consists of 9-node plane elements with element sizes of 2.5mm around the damage zone and 5mm elsewhere.

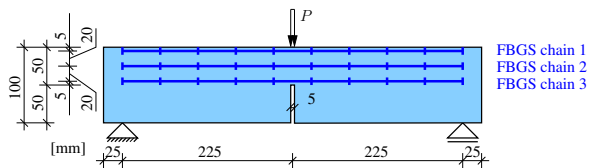


Figure 5: Geometry of notched beam and position of FBGS (fibre bragg grating sensor) chains.

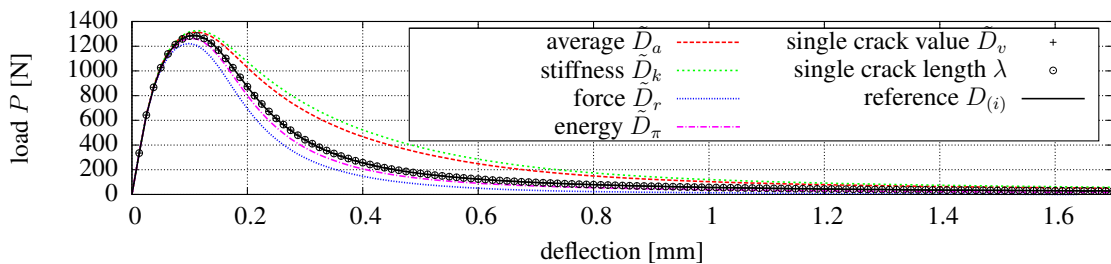


Figure 6: Comparison of load-deflection-curves for investigated simplified damage models of the notched beam.

Table 1: Parameter combinations of material and damage law obtained by model updating according to [9].

parameter	unit	value
Young's modulus E	$[10^{10} \frac{\text{N}}{\text{m}^2}]$	2.1262
Poisson's ratio ν	[-]	0.3000
compression strength f_c	$[10^7 \frac{\text{N}}{\text{m}^2}]$	4.3726
tensile strength f_t	$[10^6 \frac{\text{N}}{\text{m}^2}]$	2.5491
α	[-]	0.9790
β	$[10^2]$	1.1987
density ρ	$[10^3 \frac{\text{kg}}{\text{m}^3}]$	2.0448
$l_c = \sqrt{c}$	[mm]	1.0000

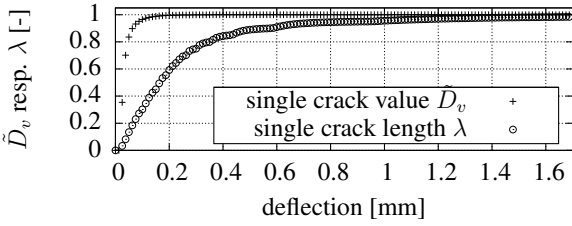


Figure 7: Damage variable history for artificial damage pattern descriptions of the notched beam.

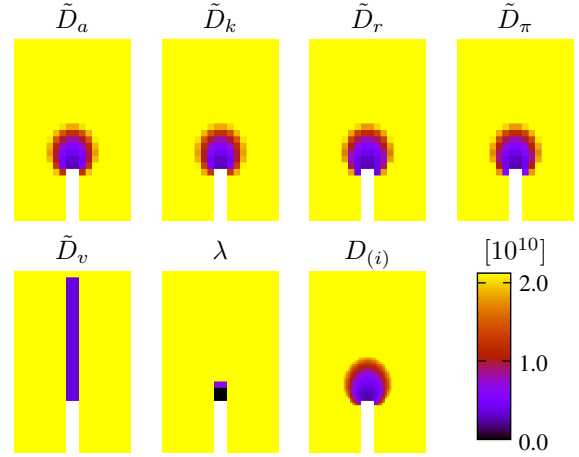
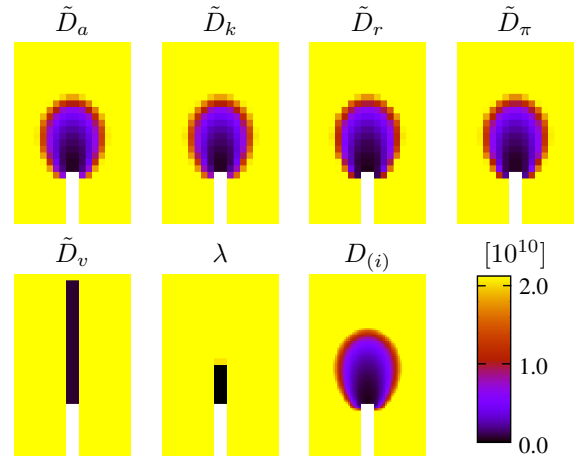
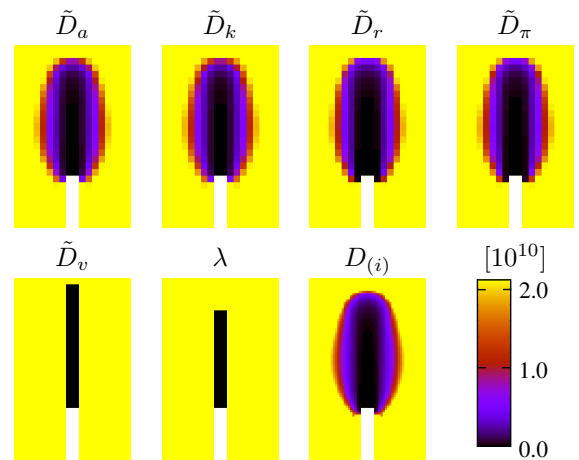
4.2 Global load-deflection-curve

By applying the approaches introduced in Section 3 to generate a finite element model with a simple linear elastic material law, the global load-deflection-curves visualised in Figure 6 can be obtained. With both artificial damage pattern approaches, a perfect fit of the global load-deflection-curve can be obtained. Of course, the parameters are optimised with respect to this load-deflection-curve.

If the true damage pattern is taken into account, the criterion using the minimised elastic potential energy yields the best agreement with respect to the global load-deflection-curve.

4.3 Local damage pattern

Figures 8, 9, and 10 show the obtained damages patterns in terms of the Young's modulus distribution for all applied simplification approaches at different damage states. For all approaches (\tilde{D}_a , \tilde{D}_k , \tilde{D}_r , \tilde{D}_π), where the damage pattern is assumed to be known, the differences are very small. Of course, the artificial patterns (\tilde{D}_v , λ) differ a lot more from the reference damage pattern. The history of the optimal damage's value and length for the description of the artificial damage patterns is given in Figure 7.


 Figure 8: Young's modulus distribution around the crack for the reference $D_{(i)}$ and all simplification approaches resulting in a deflection of 0.05mm.

 Figure 9: Young's modulus distribution around the crack for the reference $D_{(i)}$ and all simplification approaches resulting in a deflection of 0.1mm.

 Figure 10: Young's modulus distribution around the crack for the reference $D_{(i)}$ and all simplification approaches resulting in a deflection of 0.3mm.

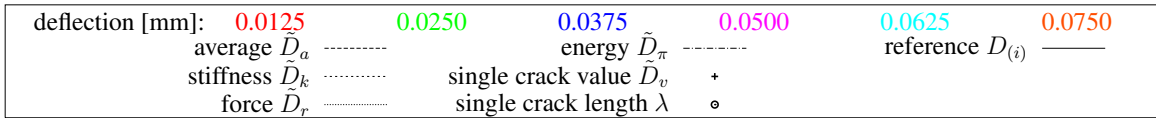
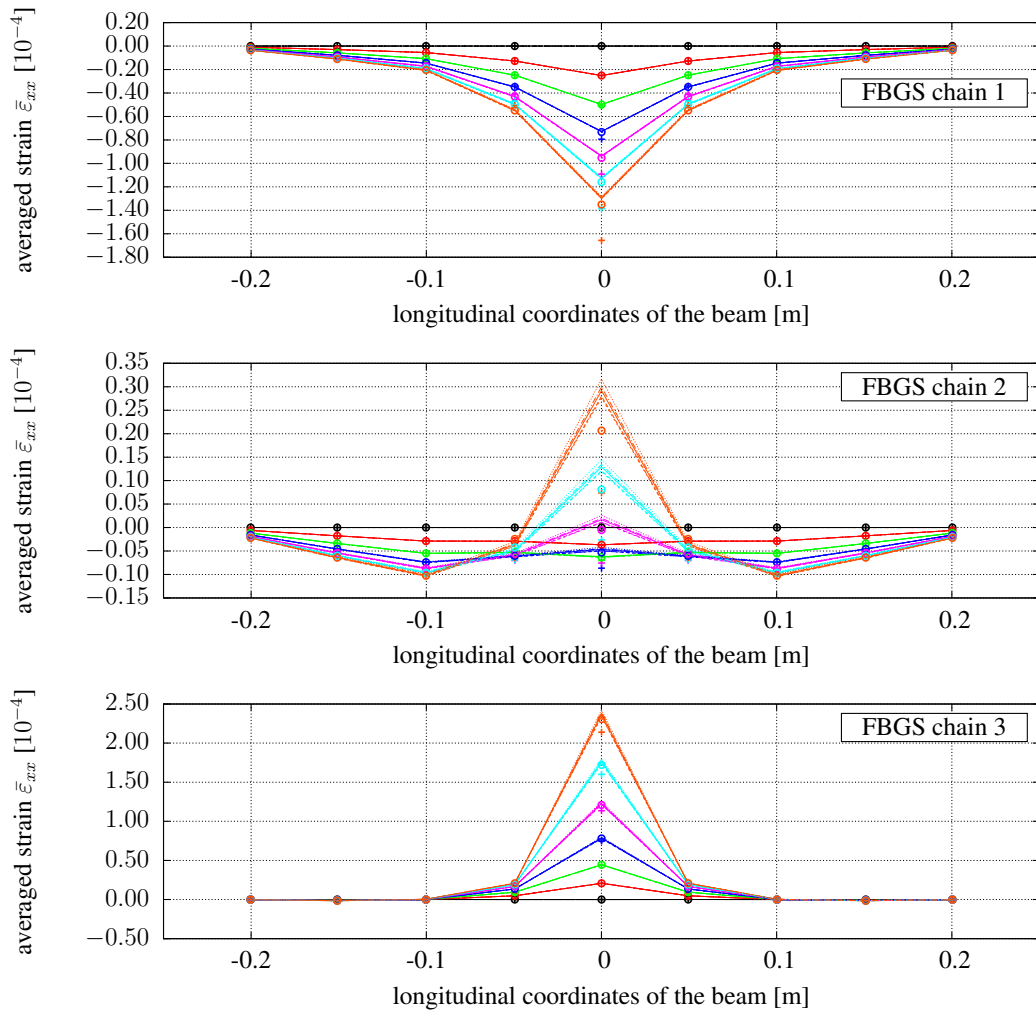


Figure 11: Distribution of averaged strains along the longitudinal axis of the beam at different heights of the cross-section.

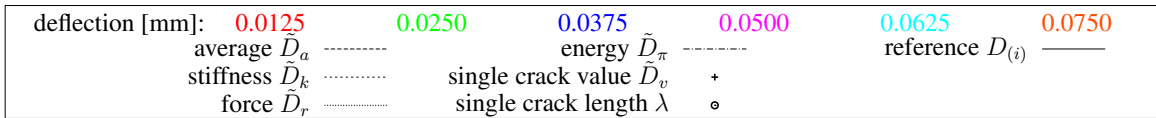
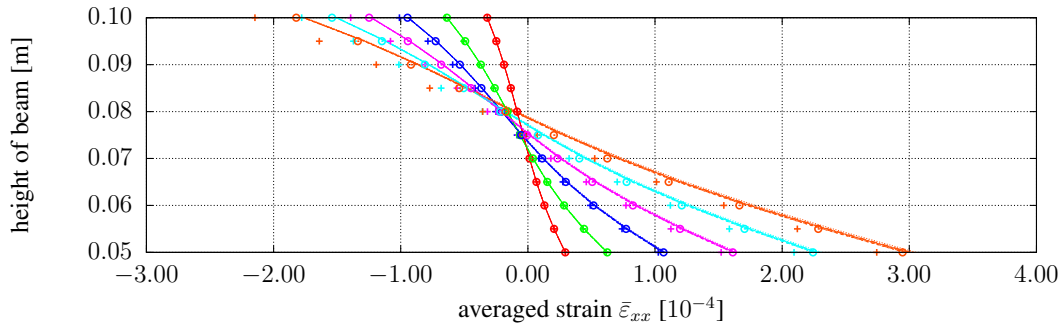


Figure 12: Distribution of the averaged strains in the central cross-section of the beam.

4.4 Averaged strains

The measures of interest in this benchmark study are the horizontal strains in the beam, which could be measured for example by FBGS (fibre bragg grating sensor) chains as indicated in Figure 5. The averaged strains using a strain gauge length of 5cm at different heights of the beam are presented in Figure 11 with progressing damage. It can be observed that all simplifications related to the realistic damage pattern show an almost perfect agreement with the reference. Also the artificial damage pattern description using the length definition of the crack shows an acceptable result at least for early damage states.

Figure 12 depicts the averaged strain distribution in the central cross-section of the beam with a gauge length of 5cm. The size of discrepancy in relation to the reference solution depends clearly on the position of the strain gauge within the beam's cross-section.

5 BENCHMARK: SIMPLY SUPPORTED BEAM

5.1 System description

The possibilities to simplify a multiple crack pattern are investigated by a simply supported plain concrete beam with a cross-section of 10cm by 10cm. Its material and damage law parameters are given in Table 1. Multiple cracks are initiated by reducing the tensile strength to 50% of the original value at the predamaged areas, indicated in Figure 15. A finite element model with quadratic 9-node plain elements of size 5mm, refined to 2.5mm around the damaged areas, is applied for the numerical calculations.

The load-deflection-curve, presented in Figure 16, is related to the vertical deflection at the position of the load application. Figure 17 depicts the damage patterns at various load steps of the reference solution obtained by the implicit gradient damage law.

5.2 Global load-deflection-curve

The criteria described in Section 3 are applied to generate the global load-deflection-

curves of the simplified linear models, which are summarised in Figure 16. In general, the results are very similar to those observed for the notched beam. If the reference damage pattern is assumed to be known, the smallest discrepancies are obtained by following the energy criterion approach. In terms of the artificial damage patterns, a single crack and a multiple crack approach are tested. For both approaches suitable values can be found to follow exactly the global load-deflection-curve of the reference solution at each load step.

5.3 Local damage pattern

By applying the approaches that assume a known damage pattern according to Subsections 3.2 and 3.3, very similar damage distributions can be obtained in comparison to the reference solution. The example for the optimal energy approach in case of load step 65 is presented in Figure 18.

Figure 18 shows also the damage patterns for the artificial damage model approach using a constant value for the whole cross-section and using a length parameter to define the damage progress. The evolution of the damage variables \tilde{D}_v and λ in dependency of the deflection is visualised in Figure 13.

It can be observed that it is important to relate a certain percentage of damage to the applied underlying damage model. For example, a damage of 20% related to the single crack approach where the severity of damage is adjusted for the whole cross-section indicates a small damage, while a damage of 20% related to the multiple crack approach described by the length of the crack indicates the ultimate load state of the structure.

Moreover, the adjustment of suitable damage levels for the artificial damage models is very difficult, if no global load-deflection-curve is available.

5.4 Averaged strains

Next to the global load-deflection-curve, averaged strains along the FBGS (fibre bragg grating sensor) chains are investigated with respect

to the simplified linear representations of the damage pattern as presented in Section 3. The positions of the FBGS chains are described in Figure 14. From the practical point of view, strains can be only measured with respect to a certain distance, which leads then to an averaged strain. Several strain gauge lengths are possible for FBGS chains. In this benchmark study, 5cm (chain 1a and 2a) and 20cm (chain 1b and 2b) strain gauge length are assumed at different heights of the beam.

In Figure 19, the comparison of the averaged strains for each FBGS position and gauge length is demonstrated for the investigated simplified damage approaches at several load steps (LS). LS 15 is related to a linear undamaged state, while LS 65 represents the peak of the global load-deflection-curve. Of course, for structural health monitoring systems, small damages as represented by LS 45 or LS 55 are of higher importance. In general, the observed discrepancies are smaller, if a 20cm gauge length instead of a 5cm gauge

length is applied. Unfortunately, a larger average length leads to a reduced significance with respect to the damage. All simplification approaches, assuming a known damage pattern, show almost identical averaged strains for the considered load steps. Only the approach following the energy criterion is representatively presented in Figure 19. The curves based on artificial damage patterns agree well with the reference curves for lower load steps until LS 45.

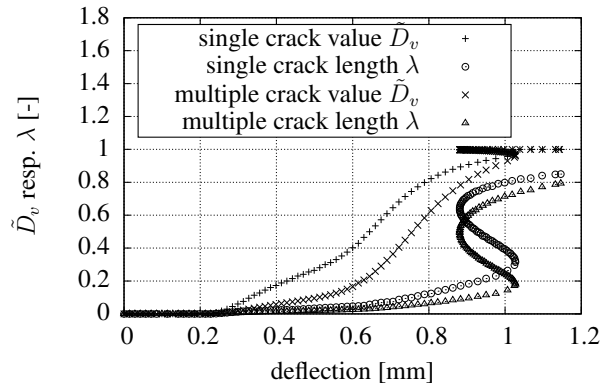


Figure 13: Damage variable history for artificial damage pattern descriptions of the simply supported beam.

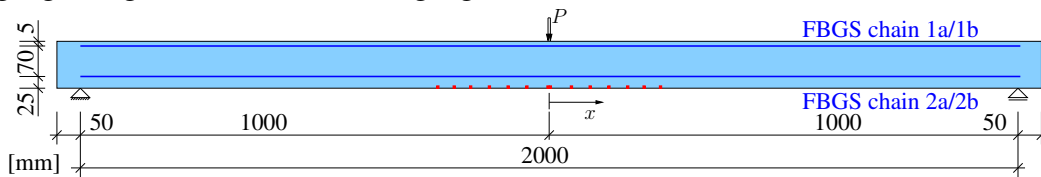


Figure 14: Geometry of investigated simply supported plain concrete beam with static loading.

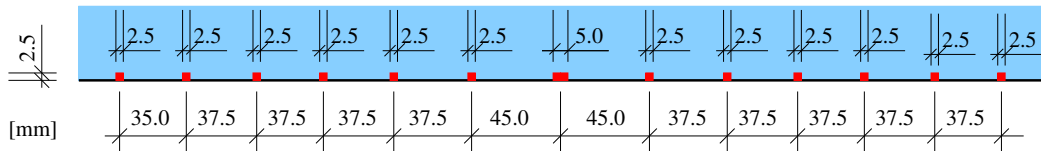


Figure 15: Detail of predamaged area.

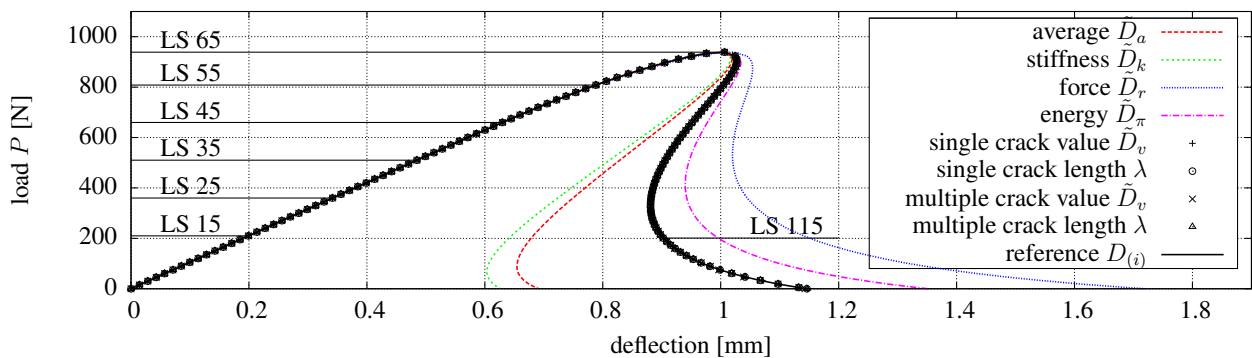


Figure 16: Comparison of load-deflection-curves for investigated simplified damage models of the simply supported beam.

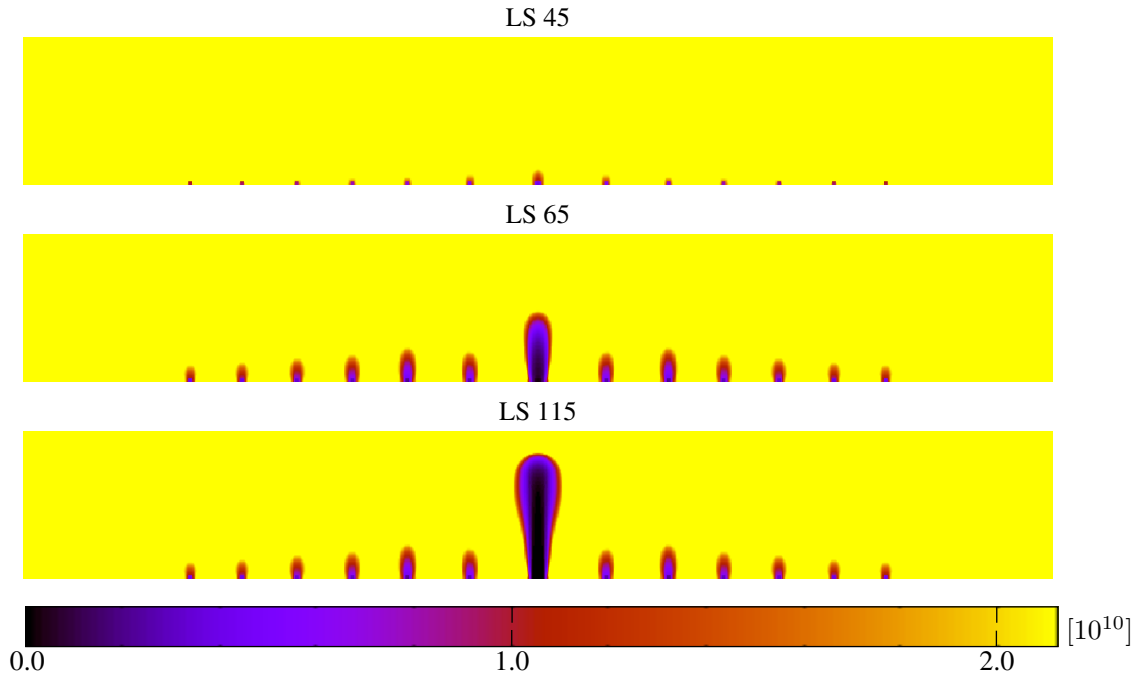


Figure 17: Young's modulus distribution around the cracks for the reference solution D_i using the implicit damage law for load steps (LS) 45, 65, and 115.

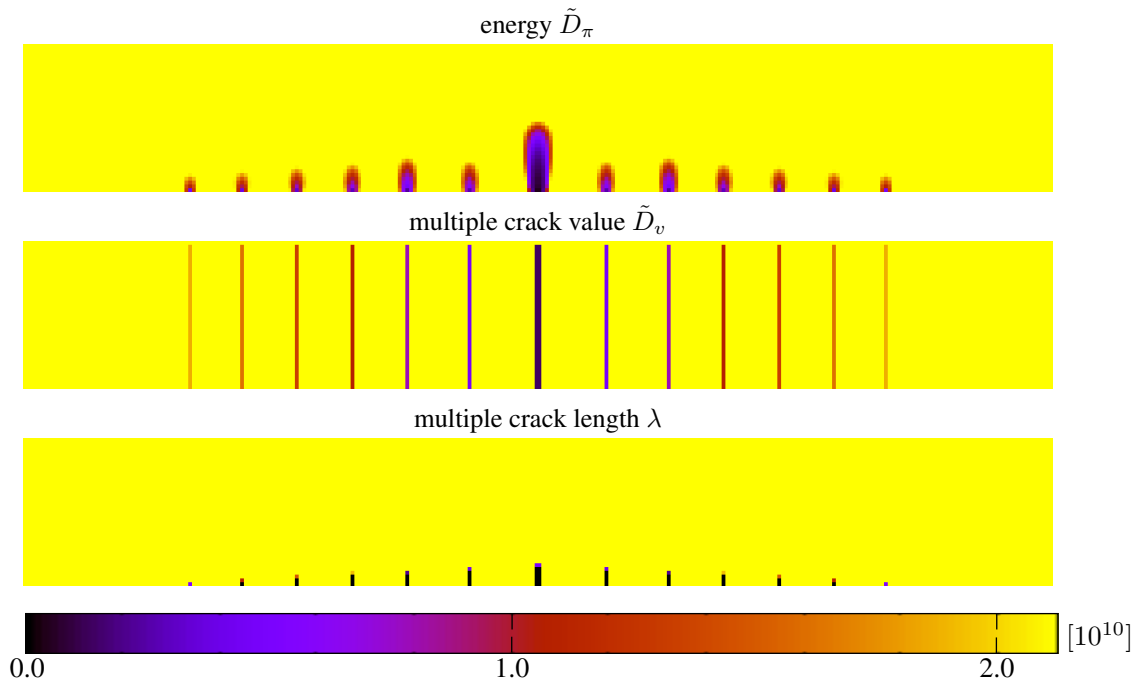


Figure 18: Young's modulus distribution around the cracks for selected investigated simplifications at load step LS 65.

6 CONCLUSIONS

This paper investigated approaches to simplify the modelling of cracks in a concrete structure. Computationally expensive damage propagation methods using the implicit damage framework and very simple damage models

typically applied in the field of vibration-based structural health monitoring were compared. A notched beam with a single crack and a simply supported beam with multiple cracks have been investigated.

The investigations showed that even very

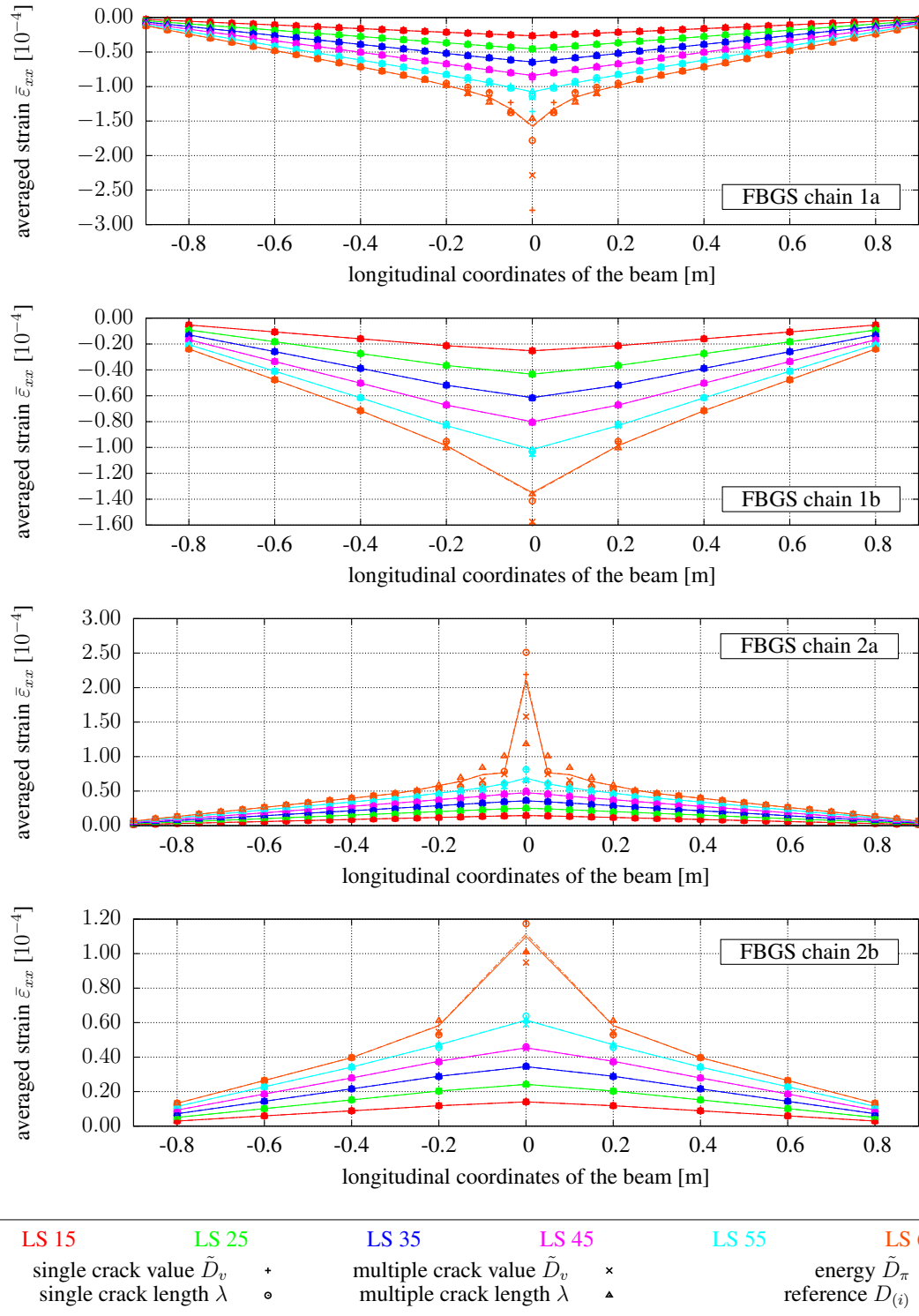


Figure 19: Distribution of averaged strains along the longitudinal axis of the beam at different heights of the cross-section for 5cm (1a/2a) and 20cm (1b/2b) gauge lengths.

simple damage pattern models, such as a constant damage over the cross-section, can be applied to represent the global behaviour of the structure as demonstrated by the global load-deflection-curves. Also the averaged strains re-

sulting from very basic descriptions of the damage pattern led to similar results in comparison to the computationally expensive reference solution, if small damages have been the subject of interest and if the averaging length has

been sufficiently large. By applying simplified damage modelling approaches, the adjustment of the severity of damage turned out to be cumbersome, if no reference solution is available.

The current comparison was limited only to static strains resulting from three-point loading tests. In vibration-based structural health monitoring systems dynamic strains are of interest, which are the input values of various features indicating the health of the structure. As the error propagation is handled differently in each feature, further research is needed to justify generally the application of simplified damage models. In addition, different loading conditions might of interest in future.

REFERENCES

- [1] T. Most. *Stochastic crack growth simulation in reinforced concrete structures by means of coupled finite element and meshless methods*. PhD thesis, Bauhaus University Weimar, Germany, 2005.
- [2] G. Hofstetter and G. Meschke, editors. *Numerical Modeling of Concrete Cracking*, volume 532 of *CISM International Centre for Mechanical Sciences*. Springer, 2011.
- [3] G. Pijaudier-Cabot and Z. P. Bazant. Non-local damage theory. *Journal of Engineering Mechanics*, 113:1512–1533, 1987.
- [4] R. H. J. Peerlings. *Enhanced damage modelling for fracture and fatigue*. PhD thesis, Eindhoven University of Technology, Eindhoven, The Netherlands, 1999.
- [5] A. Deraemaeker, E. Reynders, G. De Roeck, and J. Kullaa. Vibration based structural health monitoring using output-only measurements under changing environment. *Mechanical Systems and Signal Processing*, 22(1):34–56, 2008.
- [6] A. Teughels, J. Maeck, and G. De Roeck. Damage assessment by fe model updating using damage functions. *Computers & Structures*, 80(25):1869 – 1879, 2002.
- [7] G. Tondreau and A. Deraemaeker. Damage localization in bridges using multi-scale filters and large strain sensor networks. In *Proceedings of International Conference on Noise and Vibration Engineering ISMA, September 20-22, 2010*.
- [8] A. Deraemaeker. Assessment of damage localization based on spatial filters using numerical crack propagation models. In *Proceedings of 9th International Conference on Damage Assessment of Structures (DAMAS), July 2011, Oxford, UK, 2011*.
- [9] M. Brehm, T. J. Massart, and A. Deraemaeker. Towards a more realistic representation of concrete cracking for the design of SHM systems: updating and uncertainty evaluation of implicit gradient cracking models. In *6th European Workshop on Structural Health Monitoring, July 3 – 6, Dresden, Germany, 2012*.
- [10] M. Brehm, T. J. Massart, and A. Deraemaeker. Application of an updated notched beam model using an implicit gradient cracking approach for the purpose of damage detection based on modal strains. In *Proceedings of International Conference on Noise and Vibration Engineering (ISMA), September 17 – 19, Leuven, Belgium, 2012*.
- [11] J. H. P. de Vree, W. A. M. Brekelmans, and M. A. J. van Gils. Comparison of nonlocal approaches in continuum damage mechanics. *Computers & Structures*, 55(4):581 – 588, 1995.
- [12] H. A. Körmeling and H. W. Reinhardt. Determination of the fracture energy of normal concrete and epoxy modified concrete. Report no. 5-83-18, Stevin Laboratory, Delft University of Technology, 1983.